Experimental Evaluation of a Novel Inertial Sensor Based Realtime Gait Phase Detection Algorithm

Philipp Müller[1], **Thomas Seel**[1], **Thomas Schauer**[1]
[1]Technische Universität Berlin, Control Systems Group, Berlin, Germany

Abstract – In this paper, a novel online gait phase detection algorithm is reviewed, extended and evaluated. A foot-mounted inertial measurement unit is employed, which allows barefoot application. Using only accelerometers and gyroscopes, the method can be used indoors and in the presence of magnetic disturbances. The algorithm is designed such that the sensor can be attached in an arbitrary orientation and that it will automatically adjust to the current pace. The algorithm is evaluated using an optical motion capture system as a reference. Data from more than 100 trials with healthy subjects walking barefoot and transfemoral amputees walking with shoes is analyzed. Mean recognition delays of approx. (0.1 ± 0.05) s for the toe off and approx. (0.05 ± 0.07) s for the initial contact transition are obtained. The algorithm is found to be well suited for application in active neuroprostheses in everyday life scenarios.

1 Introduction

Stroke patients with gait abnormalities can be supported by Functional Electrical Stimulation (FES) systems. In such neuroprostheses, paralyzed muscles are activated artificially in a precise temporal pattern that resembles the physiological activity of the muscles. Therefore, the gait phases have to be detected accurately and in real time [3].
The human gait cycle can be separated into different phases. Simplest definitions such as the separation into the stance and the swing phase are possible as well as detailed divisions, for example into ten different phases [4]. Here, four basic gait events and phases are considered as represented in Figure 1. The complete contact of the foot initiates the foot rest phase. Once the heel looses ground contact, the pre-swing phase begins. The swing phase starts at the toe off event and the loading response at the first ground contact.

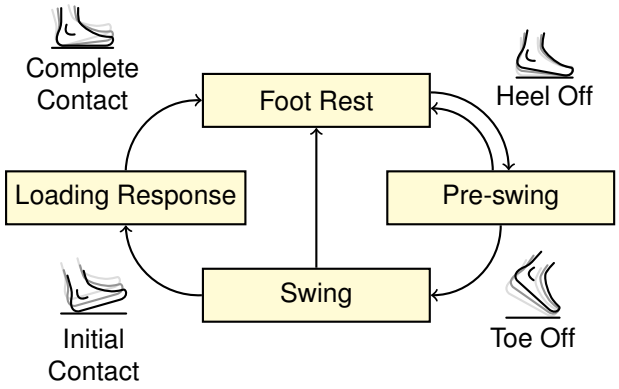

Figure 1: Gait Phase Automaton, depicting four gait phases and their transitions. During regular gate, the phases are cycled clockwise. In exceptional situations, such as sudden stops, two additional transitions to the foot rest phase may occur.

Methods for ambulatory gait phase detection include the utilization of foot switches, pressure sensor insoles, acclerometers, gyrometers and magnetometers. An extensive review can be found in [5].
Unlike other sensor systems, inertial measurement unit (IMU) can furthermore be used to estimate the body segment orientations or joint angles, see for example [7]. Such measurement information is essential in feedback-controlled neuroprostheses, such as the one in [8]. Due to this advantage, only IMU based methods are regarded in the following. Various methods have been developed, where inertial sensors wer placed on the trunk [5], the thigh [9] or the shank [10, 2, 1]. Recently, promising results where obtained in [1] where a shank-mounted IMU was used successfully to detect three different gait phases with high temporal accuracy with respect to a pressure mat system.
In this paper, we focus on gait phase detection in feedback-controlled drop foot neuroprostheses. This implies that measurements of the ankle joint angle or the foot-to-ground angle are required. Therefore, we assume that a foot-mounted IMU, consisting of a 3D accelerometer and a 3D gyroscope, is used. Unlike the commonly used heel switches and pressure soles, the IMU can easily be strapped to the instep of a shoe or bare foot. This simplifies the use of the neuroprostheses in everyday life scenarios, where the subject spends time at home wearing different or no shoes. However, it also entails that the sensor-to-foot orientation is not precisely known.

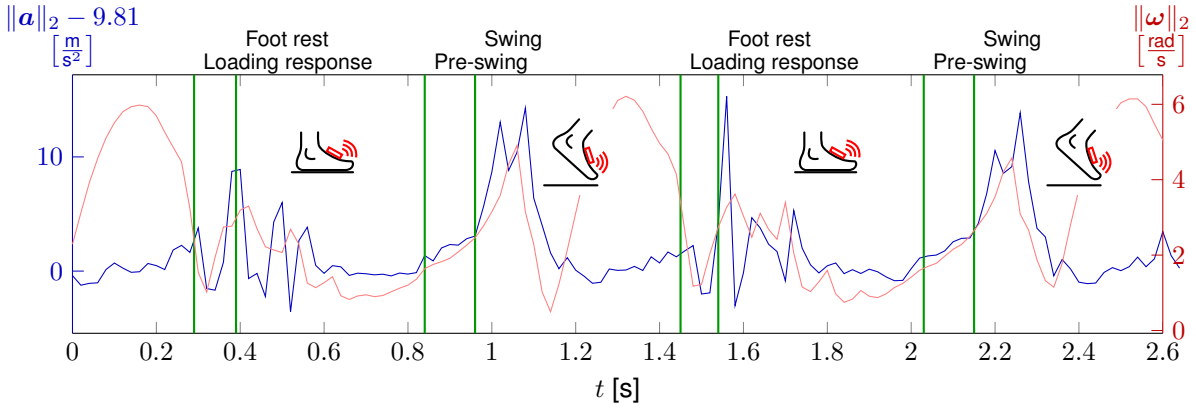

Figure 2: Norms of a foot mounted IMU measurement and corresponding gait phases. The vertical lines mark the gait phases obtained by an optical motion tracking system. The task of the IMU-based gait phase detection system is to detect the marked phases from $\boldsymbol{a}$ and ω.

An algorithm is reviewed and further developed which can detect four gait phases in real time and adapts automatically to the subject's pace. In Figure 2, the data of a typical IMU measurement is shown (note that the IMU provides a three dimensional $\boldsymbol{a}$ and $\boldsymbol{\omega}$ but the norms where plotted for better readability). It is now up the algorithm to detect the correct current gait phase, using only $\boldsymbol{a}$ and $\boldsymbol{\omega}$.
In order to assess the quality, robustness and timing of the proposed algorithm, an evaluation has to be conducted. The evaluation should consider different walking speeds as well as subjects walking with shoes and barefoot. A reference gait phase has to be obtained to detect delays and errors.

2 Proposed Algorithm

The algorithm detects the four individual gait phases described in Section 1. During regular gait, those four phases are sequentially passed. Regarding paretic gaits as well as sudden stopping, more transitions are possible. These transitions and gait phases are modeled using a finite state automaton, as shown in Figure 1. Only the transitions shown in the automaton are expected by the algorithm during a certain gait phase, for example going from swing to pre-swing is not considered possible.
In the following, the conditions for the gait transitions will be introduced. Subsequently, dynamic adaptations of the parameters to gait velocity changes will be described.

2.1 Complete Contact

Intuitively, when the foot is in the rest phase, the accelerations as well as the angular velocities measured on the instep should be close to zero. This can also occur during the swing phase, when the foot moves with almost constant velocity and orientation for a short period of time. But only in the foot rest phase, both acceleration and angular velocity stay in low bands for a sustained amount of time. As shown in Figure 1, the foot rest phase can follow all other three phases. For the transition from the loading response phase the condition is

$$(\|\boldsymbol{\omega}(i)\|_2 < \omega_{\text{rest}} \ \wedge \ \|\boldsymbol{a}(i)\|_2 - g < a_{\text{rest}}) \quad \forall\, i \in (k - n_{\text{ff}} \ldots k), \tag{1}$$

where g is the gravitational constant, k is the current sample instant, n_{ff} is the number of samples the condition has to hold, ω_{rest} and a_{rest}) are fixed parameters and $\|\boldsymbol{x}\|_2$ is the euclidean norm of $\boldsymbol{x}$.
For the transition from all other phases, (1) changes to

$$(\|\boldsymbol{\omega}(i)\|_2 < \omega_{\text{rest}} \ \wedge \ \|\boldsymbol{a}(i)\|_2 - g < \frac{1}{2} a_{\text{rest}}) \quad \forall\, i \in (k - n_{\text{ff}} \ldots k). \tag{2}$$

Where the factor $\frac{1}{2}$ is chosen to reduce false rest phase detections.

2.2 Heel off

The foot rest phase transitions to the pre-swing phase once the heel starts lifting. Thus, a rise in acceleration and angular velocity will occur. To avoid unwanted switching, a hysteresis is introduced by increasing the thresholds by a parameter $\alpha_{\text{PS}} > 1$. Thereby, the pre-swing phase is entered when

$$\|\boldsymbol{\omega}\|_2 > \alpha_{\text{PS}}\, \omega_{\text{rest}} \ \vee \ \|\boldsymbol{a}\|_2 - g > \alpha_{\text{PS}}\, a_{\text{rest}}. \tag{3}$$

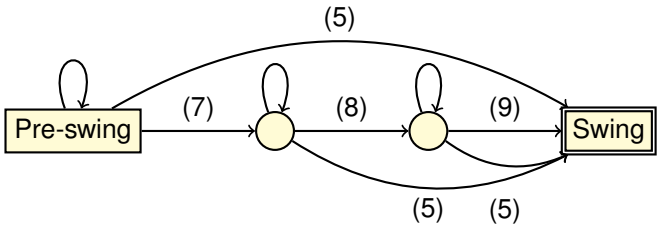

Figure 3: Recognition of the swing phase dependent on the pitch rate and toe velocity conditions (equation numbers)

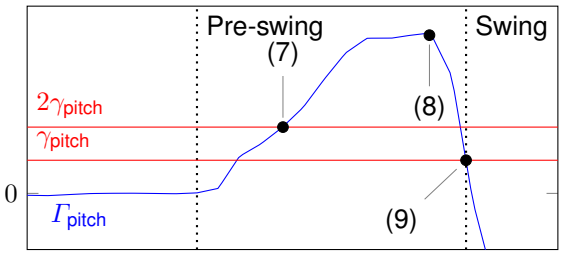

Figure 4: Typical example of the pitch rate in the pre-swing phase. Markers show when the conditions (equation numbers) are fulfilled

2.3 Toe Off

At toe off, two noticeable events occur,

1. The velocity of the IMU changes from a small to a higher value
2. The pitchrate of the foot changes from a large positive to a negative or small value, since the foot now starts to lift.

In order to integrate the IMU acceleration, it is rotated into a steady global coordinate system. Here, the rotation of the global coordinate system is defined as the rotation of the sensor at foot rest. The matrix $R(t)$, describing the current rotation of the foot can be obtained by integrating $\boldsymbol{\omega}$ via strap-down integration [6]. The integration is started at the end of the foot rest phase and reseted in all following foot rest phases. The IMU velocity is then defined as

$$\boldsymbol{v}(t) = \int_{t_0}^{t} R(\tau)\boldsymbol{a}(\tau) - \boldsymbol{a}(t_0)\, d\tau. \tag{4}$$

The swing phase is entered when

$$\|\boldsymbol{v}\|_2 > v_{\text{limit}}. \tag{5}$$

The pitch rate is the rotation caused by foot and knee flexion and extension. Here the rotation axis of the pitch rate is approximated by the average rotation axis since the last foot rest phase. The pitch rate is then the part of angular velocity around this axis

$$\Gamma_{\text{pitch}}(t) = \boldsymbol{\omega}(t)^T \frac{\int_{t_0}^{t} \boldsymbol{\omega}(\tau)d\tau}{\|\int_{t_0}^{t} \boldsymbol{\omega}(\tau)d\tau\|_2}. \tag{6}$$

The pitch rate defined in (6) is positive in the pre-swing phase and becomes negative or decreases to near-zero in the swing phase. In the following, three conditions are defined to ensure that the pitch rate has reached its maximum value and is now smaller than the defined limit

$$\Gamma_{\text{pitch}}(k) > 2\gamma_{\text{pitch}} \tag{7}$$

$$\Gamma_{\text{pitch}}(k) < \Gamma_{\text{pitch}}(k-1) \tag{8}$$

$$\Gamma_{\text{pitch}}(k) < \gamma_{\text{pitch}}, \tag{9}$$

where (7) ensures that the pitch rate is close to the set limit γ_{pitch} and (8) ensures that the pitch rate is falling and has surpassed its maximum.
For the toe off detection, the three pitch rate conditions have to be fulfilled one by one, whereas the velocity condition leads to an instant detection. This can be described by the automaton depicted in Figure 3. An example of the pitch rate during pre-swing and swing phase is given in Figure 4, here the pitch rate first passes the $2\gamma_{\text{pitch}}$ threshold, then starts falling and finally falls below γ_{pitch}.
Since the recognition by pitch rate is more precise then by velocity, v_{limit} is tuned in a way, such that the velocity condition serves as a backup. This is necessary for the case that the foot is left in a near horizontal orientation during gait.

2.4 Initial Contact

When the heel or toe touches the ground, a spike in the jerk will appear, leading to the condition

$$\|\dot{\boldsymbol{a}}\|_2 > j_{\text{min}}. \tag{10}$$

Unfortunately, there can be other, even higher spikes in the jerk, especially when the subject treads lightly. Here it is important to find the correct moment when to look for a jerk spike. A minimum swing time $T_{\text{sw min}}$ is defined that has to be passed before (10) is checked.

2.5 Gait Velocity Adaption

An issue that results from increasing walking speeds is the movement of the foot during the foot rest phase. The faster the subject moves, the less still the foot will stand. Furthermore, since the sensor is attached to the shoe or skin, it behaves like a mass-damper system, taking time to settle down. This leads to bigger unwanted accelerations and velocities depending on the gait velocity, sensor mounting, footwear and more. A method is introduced to estimate the magnitude of the unwanted movements and adapt the thresholds a_{rest} and ω_{rest} accordingly.
The here called "noise" is estimated by calculating the standard deviation of a short, N_{w} samples wide window. This standard deviation is stored for the last M_s samples and the minimum value is assumed to be during the foot rest phase, given that M_s is chosen beyond the size of one step. The thresholds a_{rest} and ω_{rest} are then

$$a_{\text{rest}} = a_{\text{gain}} \min_{i \in [k-M_s,k]} {}^{N_{\text{w}}}\sigma(\boldsymbol{a}(i)), \qquad \omega_{\text{rest}} = \omega_{\text{gain}} \min_{i \in [k-M_s,k]} {}^{N_{\text{w}}}\sigma(\boldsymbol{\omega}(i)), \tag{11}$$

where ${}^{A}\sigma(b)$ is the standard deviation of the A last samples of the signal b.
The toe off event is triggered by the velocity and the pitch rate. In order to dynamically adapt the threshold of the velocity, the maximum value of the last step is calculated

$$v_{\text{max}} = \max_{\tau \in [t_0 t]} \|\boldsymbol{v}(\tau)\|_2, \tag{12}$$

where t_0 is the time at heel off. The dynamic threshold v_{limit} is then defined by the average maximum velocity value of the last N_{vt} steps

$$v_{\text{limit}} = \alpha_{\text{vt}} \frac{1}{N_{\text{vt}}} \sum_{i=k-N_{\text{vt}}}^{k} v_{\text{max}}(i). \tag{13}$$

The same approach is used for the pitch rate, where

$$\Gamma_{\text{max}} = \max_{\tau \in [t_0 t]} \Gamma_{\text{pitch}} \qquad \gamma_{\text{pitch}} = \alpha_p \frac{1}{N_\Gamma} \sum_{i=k-N_\Gamma}^{k} \Gamma_{\text{max}}(i). \tag{14}$$

For the initial contact recognition, it is crucial to adapt the minimum swing time as well as the jerk threshold to the gait velocity. For each step i, a time $T_{\text{not FR}}(i)$ is measured which is defined by the time spent in all phases but the foot rest phase. The average over the values of the N_{sw} last steps is then taken and used to determine the minimum swing time $T_{\text{not FR}}(i)$ is the time of one step i minus the time that has been spent in foot rest.

$$T_{\text{sw min}} = \alpha_T \frac{1}{N_{\text{sw}}} \sum_{i=j-N_{\text{sw}}}^{k} T_{\text{not FR}}(i), \tag{15}$$

where j is the index of the current step.
Analogously, the jerk threshold is

$$j_{\text{min}} = \alpha_j \frac{1}{N_j} \sum_{i=k-N_j}^{k} j_{\text{max}}(i), \tag{16}$$

where $j_{\text{max}}(i)$ is the maximum jerk appearing in step i.

2.6 Gyroscopic Offset Compensation

In numerous data sets, it was observed that, especially with data from barefoot walking patients, a certain offset in $\|\boldsymbol{\omega}\|_2$ was found during the foot rest phase. In order to find the offset, the average of the current $\|\boldsymbol{\omega}\|_2$ is taken over a window of size N_g. This average is stored for the last M_g time steps, where M_g should be bigger than the duration of one step to make sure the window includes at least the previous foot rest phase. The offset is then defined as

$$\omega_{\text{avg}}(j) = \sum_{i=0}^{N_g-1} \|\boldsymbol{\omega}(k-i-j)\|_2 \tag{17}$$

$$\omega_{\text{offset}} = \min_{j \in [0, M_g]} \omega_{\text{avg}}(j), \tag{18}$$

where k is the current sampling instant. For the foot rest detection (1), ω_{offset} is now subtracted from $\|\boldsymbol{\omega}\|_2$.

Experiment	Subjects	Walking Speed	Datasets
Barefoot Experiment	14	Slow (0.9 m/s) Medium (1.2 m/s) Fast (1.6 m/s)	443
Amputee Experiment	5	Medium (1.2 m/s)	62

Table 1: Key data of the two evaluation experiments

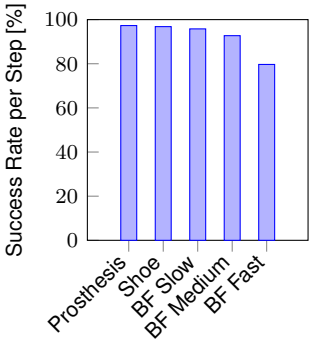

Figure 5: Bar Plot of the algorithm success rate

3 Experiment Setup

For evaluation, the recorded data of two different experiments is processed. In the first one, 14 subjects walked barefoot at three different speeds, whereas in the second one, five transfemoral amputees walked with a leg prosthesis, wearing shoes on both the prosthetic and the contralateral foot.
In both trial series, the same setup was employed: A wireless IMU was attached dorsally on the instep of each foot. Due to the wireless connection, the measured data has a sample rate of only 50Hz. Optical markers of a visual motion capture system were attached to the lateral malleolus and the head of the fifth metatarsal. Due to the limited observation volume of that system, approximately two strides per side of each subject could be recorded in the first experiment whereas in the second experiment three to four strides were possible. Each time a subject stepped through the camera array, a dataset for the left and the right foot was recorded separately. In Table 1, the details of the experiments are listed.

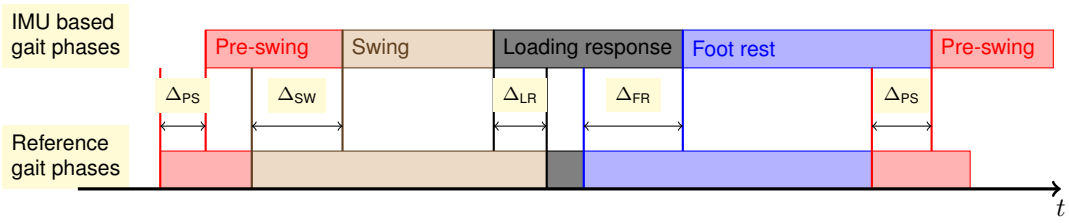

Figure 6: Example of gait phase detection delays

4 Evaluation with Respect to the Optical Reference System

In order to evaluate the proposed gait phase detection algorithm, the calculated gait phase is compared to a reference gait phase. The reference gait phase was determined using an offline algorithm that processes the vertical displacement of the optical markers on the toe and ankle. A second algorithm is used to calculate the individual delays between this reference and the gait phase detected from the inertial data. The delays obtained from a single gait cycle are visualized in Figure 6. Note that the gait phase detection delays can be negative due to early recognition.
Gait phase detection in barefoot walking subjects was found to be more challenging than for subjects wearing shoes. One of the underlying causes for this is that barefoot subjects automatically walk with a gentler initial contact, which is less painful on hard ground. The second reason is that the IMU is less stationary in the foot rest phase, since the midfoot bends as it is loaded and unloaded, as well as due to associated movements of the skin and flesh on the instep. The features described in (11), (17) and (18) helped greatly to deal with these challenges.
The success rate of the algorithm is compared in Figure 5. It can easily be seen how the walking speed affects the reliability of the algorithm. It performs significantly better in subjects wearing shoes.
In Figure 7, the delays of the four different gait phases are compared for subjects using a prosthesis, wearing shoes and walking barefoot at three different paces. It can be seen that the delays of the complete contact event have the highest value. This can be explained by the time it takes for the IMU to settle down, once on the floor. This means that, with the parameter n_{FR} set to 8, it takes approx. $n_{\mathrm{FR}} + 6$ samples to detect the complete contact.
Also it can be clearly seen, that wearing shoes leads to lower delay variances. The delays for the recognition of heel off and toe off turn out to be very short, with the toe off detection delay hardly varying at all. The rotation rate inversion of the foot happens slightly after the toe off, which explains the toe off delay.

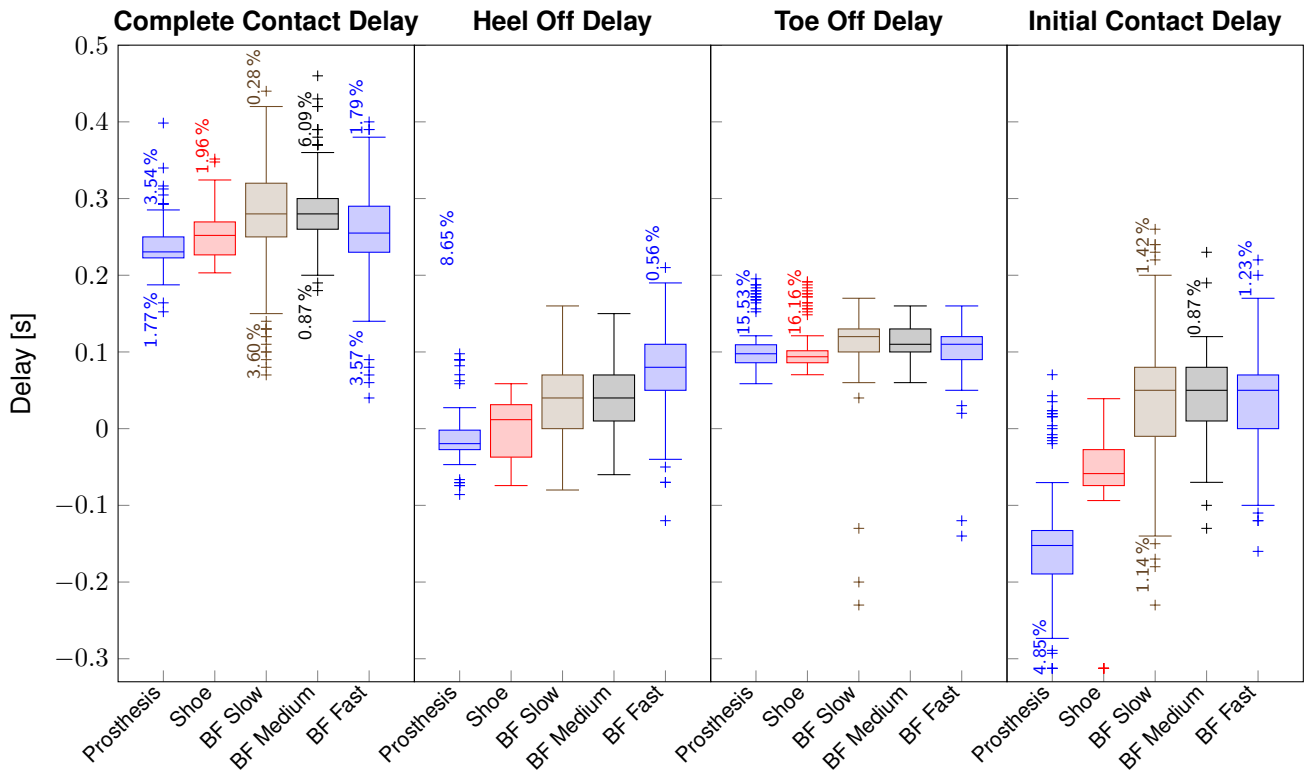

Figure 7: Box plot of the detection delays. Here, the upper and lower outliers are labeled with their percentage of the sample number. BF denotes results of the barefoot walking subjects

The toe off, as well as the initial contact delay, are important for the application in FES neuroprostheses. While the toe off leads to very satisfying results, the heel-off and initial contact recognition may be analyzed in more detail. In combination with the leg prosthesis, the majority of initial contacts were recognized to early. An investigation in the jerk progression showed a spike occuring right before the initial contact spike. A possible reason for this behavior could be the snapping of the prosthesis to its end position just before initial ground contact.
The mean delays are almost unaffected by the subject's pace, where there are big differences in the delay deviations. A medium speed seems to lead to more narrow delay deviations. Detecting complete contact as well as heel off on a prosthesis shows smaller delays and variation. This can be explained by the prosthesis being more rigid than the human foot and thus introducing less movements in foot rest.

5 Conclusion

The gait phase algorithm was thoroughly described and evaluated. Reliably detecting the gait phases of barefoot walking subjects proved to be challenging. Furthermore, the low data rate of the utilized sensor made the detection more difficult. By suitable extension of a previous algorithm, these challenges were met. Approximately 1000 individual steps over a variety of walking speeds and subjects were analyzed. Using the 3D data obtained by an optical marker system, reference gait phases were determined. Using the reference, the delays of each recognized gait phase and their statistical distributions were evaluated.
The results show, that the success rate of correctly detecting all gait phases is strongly dependent on whether the subject is wearing shoes as well as on the walking speed. Mean recognition delays of approx. 0.1 s were found for the toe off and approx. 0.05 s for the initial contact transition, with standard deviations of approx. 0.05 s and 0.07 s.
The algorithm is found to be very suitable for the application in FES-assisted gait support. Barefoot walking and higher velocities were challenging for the algorithm but still showed usable results.
In many surroundings such as indoors, magnetometers get distorted by inhomogeneous magnetic fields. The introduced algorithm exclusively utilizes accelerometers and gyroscopes and thus can be used indoors and outdoors. Together with allowing low sample frequencies for wireless transmission and the barefoot support, the algorithm can be applied in everyday life scenarios.
The observed variances of the heel off and initial contact delay will be subject of further research. Within this context, particularities in paretic and prosthetic gait will be analyzed in more detail. Furthermore, the accuracy of the employed optical gait phase estimation method will be discussed and improved.

Acknowledgments: The authors would like to thank Noelia Chia Bejarano and Simona Ferrante from Politecnico di Milano who conducted the experimental trials with barefoot walking subjects and provided the recorded data that was analyzed in this contribution. Futhermore, we gratefully acknowledge the support of Julius Thiele from Technische Universität Berlin who conducted the experimental trials with transfemoral amputees and provided the recorded data that was analyzed in this contribution.

Contact: Philipp Müller, E-Mail: mueller@control.tu-berlin.de

References

[1] N. Chia Bejarano, E. Ambrosini, A. Pedrocchi, G. Ferrigno, M. Monticone, and S. Ferrante. A novel adaptive, real-time algorithm to detect gait events from wearable sensors. *Neural Systems and Rehabilitation Engineering, IEEE Transactions on*, PP(99):1–1, 2014.

[2] D. Kotiadis, H.J. Hermens, and P.H. Veltink. Inertial gait phase detection for control of a drop foot stimulator: Inertial sensing for gait phase detection. *Medical Engineering & Physics*, 32(4):287 – 297, 2010.

[3] G.M. Lyons, T. Sinkjaer, J.H. Burridge, and D.J. Wilcox. A review of portable fes-based neural orthoses for the correction of drop foot. *Neural Systems and Rehabilitation Engineering, IEEE Transactions on*, 10(4):260–279, Dec 2002.

[4] Jacquelin Perry MD and Judith Burnfield PhD PT. *Gait Analysis: Normal and Pathological Function*. Slack Incorporated, second edition edition, 2 2010.

[5] Jan Rueterbories, Erika G. Spaich, Birgit Larsen, and Ole K. Andersen. Methods for gait event detection and analysis in ambulatory systems. *Medical Engineering & Physics*, 32(6):545 – 552, 2010.

[6] Paul G Savage. Strapdown inertial navigation integration algorithm design part 1: Attitude algorithms. *Journal of guidance, control, and dynamics*, 21(1):19–28, 1998.

[7] T. Seel, Daniel Laidig, Markus Valtin, Cordula Werner, Jörg Raisch, and Thomas Schauer. Feedback control of foot eversion in the adaptive peroneal stimulator. In *Proceedings of the 22nd Mediterranean Conference on Control and Automation*, page 1482–1487, Palermo, Italy, 2014.

[8] T. Seel, S. Schäperkötter, M. Valtin, C. Werner, and T. Schauer. Design and control of an adaptive peroneal stimulator with inertial sensor-based gait phase detection. In *18th Annual International FES Society Conference*, pages 177–180, San Sebastian, Spain, 2013.

[9] Yoichi Shimada, Shigeru Ando, Toshiki Matsunaga, Akiko Misawa, Toshiaki Aizawa, Tsuyoshi Shirahata, and Eiji Itoi. Clinical application of acceleration sensor to detect the swing phase of stroke gait in functional electrical stimulation. *The Tohoku Journal of Experimental Medicine*, 207(3):197–202, 2005.

[10] R. Williamson and B.J. Andrews. Gait event detection for fes using accelerometers and supervised machine learning. *Rehabilitation Engineering, IEEE Transactions on*, 8(3):312–319, Sep 2000.